Available online at www.sciencedirect.com

ScienceDirect

Materials Today: Proceedings 4 (2017) S12–S18

materialstoday: PROCEEDINGS

www.materialstoday.com/proceedings

EMRS 2016

Superlinear emission in bare perovskite: amplified spontaneous emission in disordered film versus single crystal lasing*

F.Biccari[a], F.Gabelloni[a], C.Francioni[a], F.La China[a], N.Caselli[a], F.Intonti[a], M.Gurioli[a], J.Lee[b], S.Leblebici[b], A. Weber-Bargioni[b] and A.Vinattieri[a]*

[a] *Department of Physics and Astronomy, LENS, University of Florence,50019 Sesto Fiorentino, Italy*
[b] *Molecular Foundry, Lawrence Berkeley National Laboratory, Berkeley, USA*

Abstract

We present an experimental study concerning the superlinear emission in organic-inorganic halide perovskites. Microphotoluminescence experiments under CW and picosecond excitation condition at low temperature and near field optical photoluminescence spectra at room temperature provide clear evidence of the very different origin of the superlinear regime in disordered films and microplates/microwires. Insights on the origin of modal structures of the emission spectra in the high excitation regime will be given by polarization-resolved photoluminescence experiments.

Selection and Peer-review under responsibility of conference committee members of EMRS 2016 symposium Light interaction with nanomaterials.

Keywords: perovskites;microphotoluminescence; near field spectroscopuy; lasing.

1. Introduction

In the last decade a significant effort of research in the field of physics and chemistry has been directed to the development and study of organic-inorganic materials for photonics and energy harvesting applications.

* Corresponding author. Tel.: +39-055-4572049; fax: +39-055-4574914.
E-mail address: vinattieri@fi.infn.it

From this side, perovskites represent a class of materials of extreme relevance [1], since their composition and design can be tuned in quite a wide range to satisfy requirements as:

- very high absorption coefficient and high efficient radiative recombination, being a direct bandgap material,
- tunability of the emission to cover the visible range,
- design of the material structure, from bulk to ordered microstructures or to disordered films with different optical properties,
- easiness of realization which is an important issue for device realization and future large-scale applications, even though long term sample stability is still challenging.

More recently, metal-halide perovskites have received the interest of the scientific community because of the outstanding results obtained with their use as absorbing material in solid-state solar cells [2-4]. At the same time a dramatic increase of the emission intensity and narrowing of the spectrum [5] has been demonstrated in microwires and microplates [6] and in disordered films [7]. Despite these results and the rapid progress in both photonics and energy harvesting applications of perovskites, there is still a lack of knowledge and understanding of the main microscopic mechanisms and processes that rule the carrier relaxation and recombination in such materials. In this paper we present a detailed experimental investigation of $CH_3NH_3PbI_3$ (hereafter indicated as MAPI) bare films (BF) and microwires (MWR) on quartz substrates by means of microphotoluminescence and near field optical spectroscopy under continuous wave (CW) and picosecond excitation conditions.

2. Experimental and Results

MAPI microwires (MWR) samples were grown following the procedure reported in [6]. A lead acetate dihydrate/dimethyl sulfoxide solution at a concentration of 100 mg/ml was drop-cast on a quartz substrate treated with oxygen plasma and annealed at 60 ^{0}C on a hot plate for ~30 minutes. The lead acetate film was immersed in 2 ml of MAI/IPA solution at a concentration of 30 mg/ml at room temperature for ~24 hours in a nitrogen glove box. Films of bare MAPI (BF) were also prepared and deposited on quartz substrate.
Samples were placed in a cold-finger helium flow cryostat and micro-PL measurements were performed in the far field using a confocal microscope equipped with a infinity corrected objective (numerical aperture 0.5) assuring a lateral resolution of 0.7 μm and dispersed by a single grating spectrometer with 250 μeV spectral resolution. CW excitation was provided by a doubled Nd:YAG laser at 532 nm while, for time-resolved experiments, femtosecond excitation was realized doubling 0.2 ps pulses of a Ti: Sapphire laser at 800 nm and 82 MHz repetition rate. Time-correlated single photon counting was implemented with an APD providing ≈30 ps time–resolution. Optical spectra in near field and topographic maps were obtained by a commercial Twin-SNOM by Omicron, operating at room temperature and exciting the sample with a CW He-Ne laser at 633 nm. The spatial resolution of the SNOM setup with the dielectric tip used in the experiments is ≈250 nm.
In fig.1a,b typical micro-PL spectra at 10 K in the low excitation regime along with SNOM maps are reported for the BF and MWR samples where isolated wires are easily detectable. The spatial scale of the roughness in the disordered film is a few tens of nm and, in the micro-PL spectra, the BF emission is strongly dependent on the selected region of the sample not only for what concerns the intensity but also for the relative contribution of the tetragonal/orthorhombic band. In fact despite at low T the crystalline phase is orthorhombic, tetragonal inclusions have been already observed in literature [8]. Instead, room temperature PL spectra (Fig.1c,d)) realized with the SNOM microscope show only little variation in the PL band, even when scanning regions of tens of microns with a resolution of ≈250 nm.

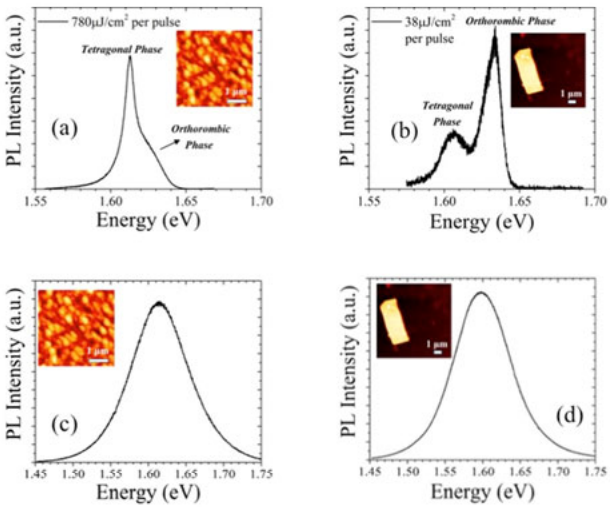

Fig.1: PL spectra at 10 K of the film (BF) (a) and microwire (MWR) (b) in the low excitation density regime. In the insets typical SNOM topography maps are shown. (c) SNOM PL spectra at 300K after CW excitation at 633 nm of the film (c) and microwire (d).

In fact at 300 K, scanning with the SNOM probe, emission from the tetragonal phase is observed both from the film and the wires with similar broadening and no remarkable spectral difference in the submicrometric spatial scale, apart from intensity fluctuations. From SNOM topography, in the MWR sample each single microwire shows an homogenous thickness in the micrometer scale but the low T PL spectra still display a significant inhomogeneous broadening with the dominant emission of the orthorhombic phase (as expected at low T) with a residual contribution from tetragonal inclusions. Hereafter we will indicate such broad band observed from BF and MWR samples as spontaneous emission (SPE).

Typical PL spectra at 10 K are shown in fig.2 for the BF (left side) and a MWR (right side). I_0 corresponds to an excitation density of 780 μJ/cm^2 per pulse for the film and 57μJ/cm^2 per pulse for the microwire. A superlinear increase of the emission, when the excitation density exceeds ≈ 3.5 mJ/cm^2 per pulse for the BF and ≈80 μJ/cm^2

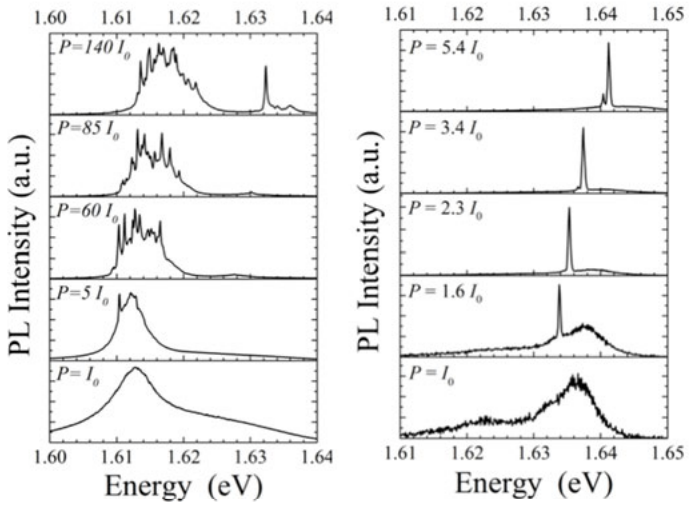

Fig.2: PL spectra at 10 K of the film (left panels) and microwire (right panels) as a function of the excitation intensity.

per pulse for the MWR, is observed, along with the appearance of multimodal features in the PL of the film and one or a few narrow peaks in the PL spectra of the microwire sample, depending on the selected micro-crystal.

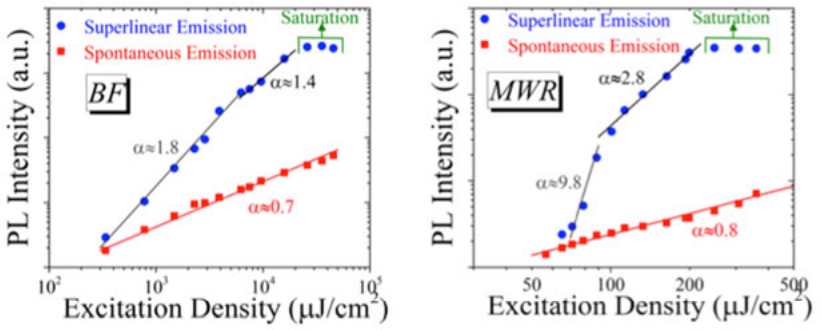

Fig.3: Dependence of the PL intensity for the BF and MWR sample on the excitation density per pulse .

In fig. 3 the power dependence of the intensity for the BF and MWR at the narrow peak (blue points) is compared with the behavior of the broad PL spectra (red squares) which turns out to be slightly sublinear while a superlinear trend is observed for the narrow peak followed by a saturation. For the BF similar dependence is found for each of the narrow peaks of fig.2. It is worth noting that the investigated range for the BF covers four decades of intensity while for the MWR, in a decade of intensity the superlinearity saturates. A blue shift of the superlinear emission (SE) is eventually observed for microwires but it is also observable in the bare film (see fig.2).

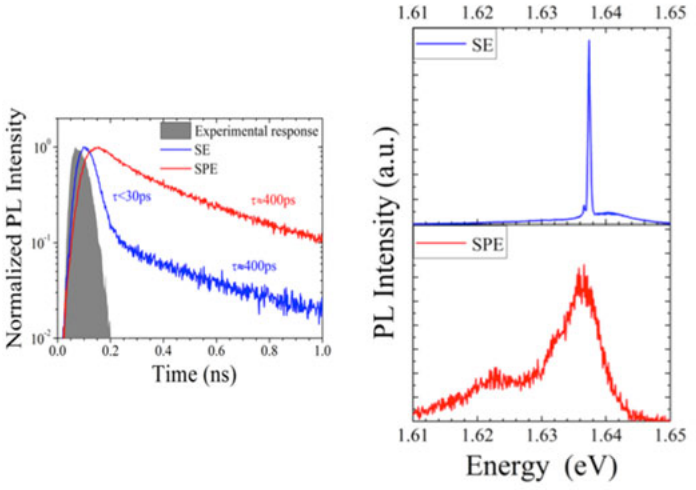

Fig.4: Time evolution of the SE and SPE signal after excitation with a 0.2 ps pulse for the microwire sample. The grey shaded area represents the experimental time response to the subpicosecond pulse. Spectra are also shown in high/low excitation condition.

The SE shows clear signature also in the time evolution of the signal. In fig.4 the decay of the SE and SPE signal is reported along with the experimental time response: it clearly appears that the SE at 1.637 eV occurs only in the first few tens of ps and the longer decay time comes from the residual SPE signal. Moreover the risetime of the SE

is almost limited by the time resolution, which is not the case for the spontaneous emission. Time evolution of the SE and SPE signals are similar for the BF and the MWR samples indicating that apparently the nature of SE is the same in both cases.
Polarization-resolved experiments were performed to clarify the origin of the superlinear emission in BF and MWRs and results are shown in fig.5.

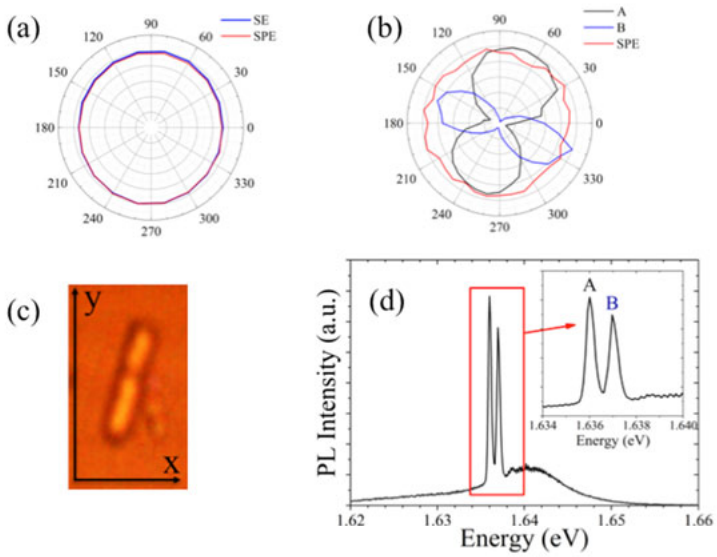

Fig.5: a) Polar diagram of the polarization of SE and SPE signals for the BF sample. b) Polar diagram of the polarization of SPE and A,B modes for MWR sample. c) image of the MWR analyzed in (b). The polarizer at 0 is aligned along x axis . d) Spectrum of the MWR (c) showing the modes A,B whose polarization is reported in (b).

The polar diagram for the PL from the film does not show any difference between the low and high excitation regime: in fact the emission turns out to be unpolarized in both cases at fixed energies in the spectrum. In particular we analyzed the polarization at the energies where narrow peaks appear at higher excitation density. On the contrary a significant polarization (≈ 80%) is detected for the superlinear emission in the MWR sample. Moreover we observed that in the case of two lines appearing in the PL, they result cross-polarized and the polarization of each line is aligned along each main axis of the sample (fig.5). Time-resolved PL measurements show that both sharp emissions of Fig.5d, after proper spectral range and polarization are chosen for each peak, have a fast decay rate followed by a slow decay rate due to the underlying signal (as already observed in Fig.4). Using the same excitation power (above the threshold) but choosing the orthogonal polarization, the remaining underlying signal shows only the slow decay rate. Therefore the polarization analysis results as the way to distinguish the nature of the SE in the bare film and the MWR sample and in the case of the MWR is related to the sample morphology. In fact in the BF sample the absence of any polarization in the SE indicates that the physical origin of the superlinear signal is the amplification of a spontaneous emission as commonly observed in random lasers [9] and it shows up in multi- pseudo-modal behavior, where each pseudo-mode corresponds to a specific path of the emitted photon in the sample. Instead the MWR behaves as a lossy microcavity, and the refractive index contrast between the perovskite wire and the vacuum (substrate) guarantees enough reflection to build up a stimulated emission under pulsed excitation. The effectiveness of the cavity in the MWR shows up in the reduced threshold for the superlinear signal respect to the BF. Moreover, given the size of the wires (1-10 μm), only few longitudinal modes can be eventually excited in the PL band. In fact we observe only a few modes and strong spatial inhomogeneity is also detected in the signal from the MWR as shown in fig.6.
In our experimental setup we excite the sample with a spot diameter ≤1 μm and collect the signal with less than one micrometer resolution: this allows for mapping the SPE and SE in different regions of each microwire. While in

the BF differences in the spectra are observed concerning the pseudo-mode distribution and onset value of the superlinear emission, in the MWR sample the SE comes from hot spots in the sample (region A) as shown in fig.6a while the SPE corresponds to the broad pedestal, more easily observed in fig.6b where the signal is collected from region B. Quite puzzling is presently the origin of the hot spots which possibly are related to diffusion /localization centers: in fact diffusion will be of help in the PL signal extraction given our experimental setup where illumination/detection occurs in the direction orthogonal to the sample plane, but exciton localization will provide a favourable condition for light amplification. Investigations are in progress to clarify this point: we remark that in

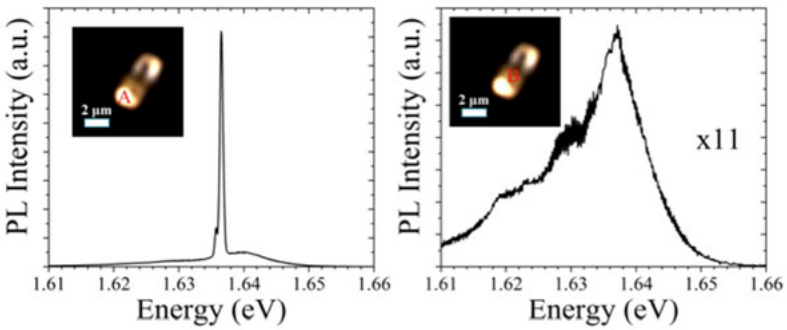

Fig.6: Micro-PL spectra in different points (A,B) of a microwire at fixed excitation density, showing the presence of an hot spot.

the low excitation regime we do not have any evidence of significant inhomogeneity in the spectrum and intensity of the spontaneous emission while they are observed only in the superlinear regime. Therefore it is unlikely that they are related to the presence of localized non-radiative centers since they will play a role also in the low excitation regime.

3. Conclusions

We have reported on the origin of the superlinear emission observed in disordered films and microwires of $CH_3NH_3PbI_3$. Micro-PL spectra acquired varying several experimental parameters clearly show that the multimode structure of the PL, observed in perovskite disordered films in high excitation condition, come from an amplified spontaneous emission typical of random lasing media. On the contrary, in microwire samples, the strongly superlinear polarized emission can be interpreted as the occurrence of a lasing regime and our results correlate clearly the polarization axis of the superlinear emission with direction determined by the sample geometry.

Acknowledgements

We warmly acknowledge Prof. F.Bogani for helpful discussions and suggestions.

References

[1] S.D.Stranks and H.J.Snaith: Nature Nanotechnology 10, 391 (2015)
[2] M. M. Lee et al.: Science 338, 643 (2012)
[3] G.Hodes:: Science 342, 317 (2013)
[4] Gratzel, M: Nature Materials 13, 838 (2014).
[5] B.R Sutherland and E.H.Sargent: Nature Photonics 10,295 (2016)
[6] Zhu, Haiming, et al. :Nature Materials 14, 636 (2015)
[7] Guichuan Xing et al: Nature Materials 13, 476 (2014)
[8] C.Wehrenfennig et al.: APL Materials 2, 081513 (2014)
[9] R.Dhanker et al.: Appl.Phys.Lett. 105,151112 (2014)